Numerical study on the thermodynamic characteristics

in a Twin Swirl pulverized coal Combustor

Yinli LIU, *†Hao TANG, Yongfen WANG

College of Energy and Power Engineering,
Nanjing University of Aeronautics and Astronautics, Nanjing 210016, China
* Presenting author: hao.tang@nuaa.edu.cn
†Corresponding author: hao.tang@nuaa.edu.cn

Abstract

Numerical simulations were conducted to study the combustion characteristics in a coaxial Twin Swirl Combustor (TSC) burning pulverized coal. Results under different stoichiometric ratios show that volatiles release in between two recirculation zones close to the secondary air inlet, and char burns mostly in the near-wall region due to the centrifugal force brought in by two swirling airflows. Intensive near-wall burning of pulverized coal favors a relatively high wall temperature, contributing to continuous molten slag discharge. An evenly distributed temperature profile with an average of about 1500 K in the chamber is obtained, which is beneficial for low NOx emissions. The case with stoichiometric ratios of 0.9 yielded lower NOx emission rates near exit while remains high volatile conversion rate and char burnout rate, as compared with the case with stoichiometric ratios of 0.8.

Keywords: Twin swirl combustor, Computational Fluid Dynamics (CFD), thermal, NOx

Introduction

Confined swirling flows are widely used in most the industrial instruments, i.e. internal combustion engines and industrial burners. A strong swirling airflow in the chamber will cause negative-pressure effects, generating internal recirculation zones (IRZ). The existence of recirculation is beneficial for both premix and non-premixed combustion. In pulverized coal combustion, it can help increase the gas recirculation for flame stabilization, and prolonging the travelling time of the coal particles, which is beneficial for reaching high-level burnout rate.

In this paper, a Twin Swirling Combustor (TSC) burning pulverized coal has been proposed. A schematic plot for the inlet structures of TSC is shown in Figure 1. With two swirling airflows, coal particles are burned near the chamber wall in intensive combustion rates. Under the centrifugal force, burnout particles are captured by the chamber wall in the form of fusion slag. With the operation pressure and/or the gravity effect, the ash is removed in the form of molten slag and discharged from the bottom of the combustor to a water quenched slag hopper, where it forms crystal pellets.

CFD simulation was conducted on the Twin Swirl pulverized coal Combustor (TSC) to evaluate the combustion performance inside the chamber in a slagging combustion condition. Results under different stoichiometric ratios were obtained in a fuel-rich condition for restraining of NOx generation. C1 and C2 were given to each case, with the stoichiometric ratio (α) of 0.9 and 0.8, respectively. Comparative analyses were

made on the combustion performance as well as the pollutant emission rates. A schematic plot for the inlet structures of TSC is shown in Fig. 1. The non-swirling inner primary and outer secondary airflows were turned into two coaxial swirling airflows with the same swirl direction after they flow through the fixed annular vanes. Detailed geometries for TSC can be referred to [Liu and Tang (2014)]. Inlet conditions for case C1 and C2 are described in Table 1. Coal proximate analyses and ultimate analyses results are illustrated in Table 2.

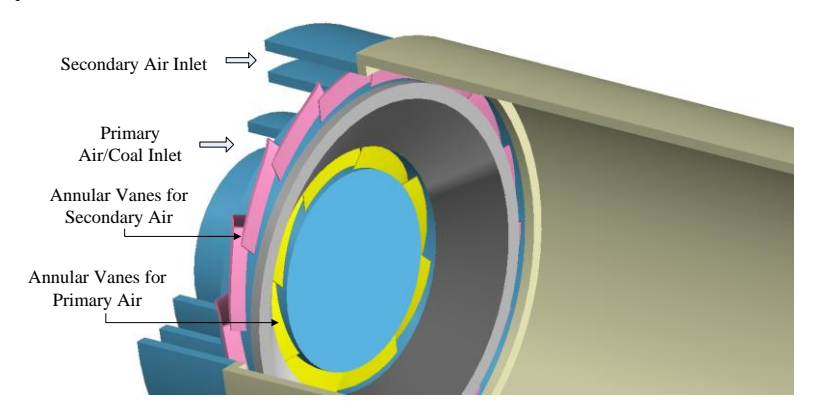


Figure 1. Schematic plot of inlet structures of TSC

Table 1 Operation conditions for different cases

	Stoichiome-	Air flow rate (kg/s)	Coal feed rate (kg/s)	Temperature (K)		
	tric ratio α			Primary air	Secondary air	
C1	0.9	5.559e-2	7.676e-3	293	673	
C2	0.8	5.559e-2	8.529e-3	293	673	

Table 2 Properties of the pulverized coal

Proximate analysis (%)				Ultimate analysis (%)				
FC	Volatile	Ash	Moisture	С	Н	O	N	S
36.9	45.5	12.9	4.7	77.58	6.57	14.71	1.12	0.02

Numerical models and mathematical methods

The thermal simulation of the pulverized coal combustion in TSC was performed using a finite volume method. Coal combustion is modeled as a diluted two-phase (solid-gas) reacting flow using an Eulerian-Lagrangian approach. For the gas phase, the governing equations of mass, momentum, species and energy are written in conservative form:

$$\frac{\partial(\rho\Phi)}{\partial t} + \frac{\partial(\rho u_j\Phi)}{\partial x_j} = \frac{\partial}{\partial x_j} \left(\Gamma_{\Phi} \frac{\partial\Phi}{\partial x_j} \right) + S_{\Phi}$$
 (1)

With Φ , t, u, Γ_{Φ} and S_{Φ} denoting Favre-averaged variables, time, velocity diffusion coefficient, and source term, respectively [Muller et al. (2010)].

The RNG k- ε model [Yakhot and Orszag (1986)] was adopted to simulate the turbulent flows in the chamber. The devolatilisation process of the coal particles was

simulated using the two-competing-rate model [Kobayashi et al. (1976)]. The turbulence-chemistry interaction was modeled using the finite-rate/eddy-dissipation model with the β -Probability Density Function (PDF) methods [Smoot and Smith (1985)]. The Discrete Ordinates (DO) model [Raithby and Chui (1990)] was used to calculate the radiation heat transfer. For the prediction of NO_x emission, both the thermal and fuel NO_x were calculated, while the prompt NO_x was ignored [Zhou et al. (2014)]. The formation of the thermal NO_x is modeled by the extended Zeldovich mechanism [Zeldovich (1946)]. Fuel NO_x is generated when nitrogen originally bound in the coal particles combines with excess oxygen.

Mesh independence test had been implemented before simulations started. A total number of about 100,000 quadrilateral mesh cells were chosen for all the calculations. The isothermal cases were first simulated with converged results. Then coal particles were added to couple with the continuous phase calculation. Convergence criteria were set to five orders of magnitude reduction and at least 20,000 iterations were carried out to ensure the convergence.

Results and discussion

The contours of the axial velocity are shown in Figure 2. Only half of the calculation domain is shown due to axisymmetric flow characteristics. The upper half depicts the axial velocity under isothermal condition, while the lower half describes the axial velocity of C2, which is under thermal condition. The recirculation zones are highlighted with black curves, in which the axial velocity is negative. The IRZ moves more downstream towards the axis direction under thermal condition, and the area of IRZ is larger compared with the isothermal one. There is another recirculation zone near the combustor wall. When combustion process is taken into consideration, this recirculation zone becomes smaller and move downstream. The discrepancy in the shape and location of the IRZ can be due to two aspects. Firstly, the chemical reactions and heat generated during coal combustion have huge impacts on the flow field inside the chamber. Also, when coal particles are added into the chamber, the interaction between the air and coal particles can also affect the aerodynamic field of the continuous phase.

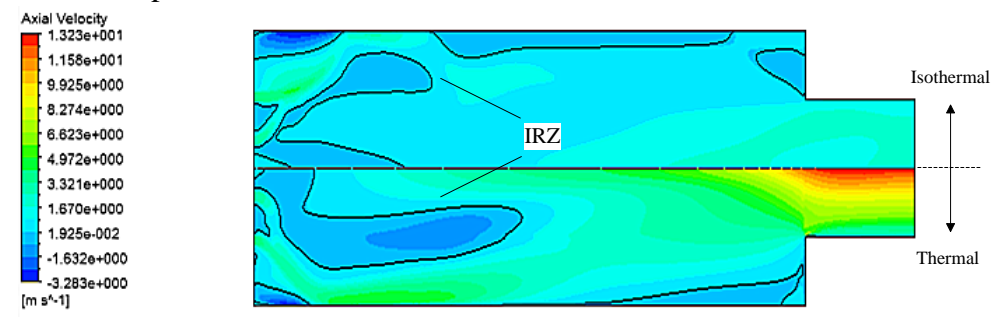


Figure 2. Contours of axial velocity (upper half, isothermal results; lower half, thermal results)

Figure 3 compares the particle evaporation/devolatilization rate and particle burnout rate for C1 and C2 are shown in Figure 4. In each figure, the upper half is the contour of C1 ($\alpha = 0.9$) and the lower half is that of C2 ($\alpha = 0.8$). The light yellow outlines in Figure 3 and Figure 4 depict the recirculation zones where the axial velocity is negative. Though the length of the IRZ of C1 is slightly larger than that of C2, the other recirculation zones are almost with same shape and located in same place. As

seen in Figure 3, the place where volatiles release from coal particles is located just in between the two recirculation zones near the secondary air inlet. Moreover, the contour of particle burnout rate shown in Figure 4 indicate that char also burns out in between two recirculation zones, though the char burnout district extends further downstream along the axial direction than that of evaporation/devolatilization zone. As is shown in Figure 3, the contours for particle evaporation/devolatilization rates of C1 and C2 differ little from each other. For C2, a higher evaporation/devolatilization rate is obtained. Similarly, higher burnout intensity is fulfilled in C2, while the length of the char burnout area of C1 is larger than that of C2. The char burnout zones for both cases are located in the vicinity of wall regions, due the centrifugal force aroused by the swirling airflows. Large evaporation/devolatilization rate and char burnout rate near the chamber wall indicates an intensive combustion in the near-wall region, which is beneficial for particle deposition and melting slag discharge.

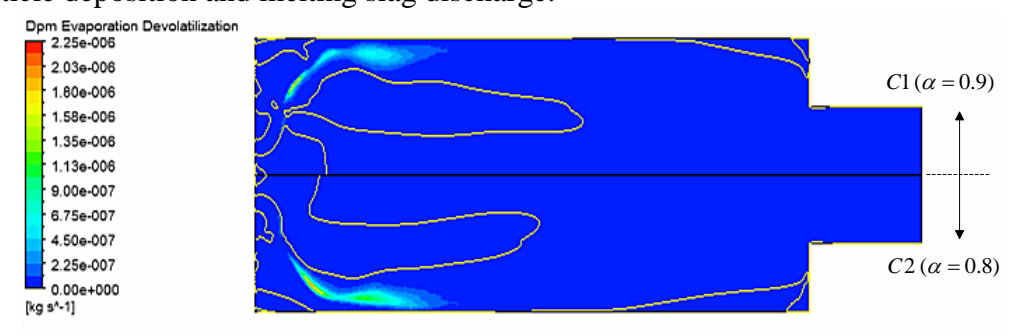


Figure 3. Contours of particle evaporation/devolatilization rate (upper half, C1; lower half, C2)

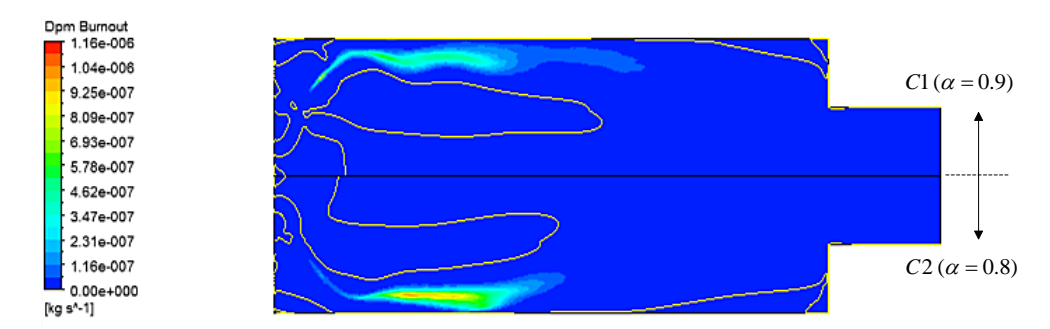


Figure 4. Contours of particle burnout rate (upper half, C1; lower half, C2)

The temperature contours in the TSC chamber of C1 and C2 are depicted in Figure 5. A relatively uniform temperature distribution is obtained, which is beneficial for low thermal NOx emission. In most part of the chamber for both cases, the temperature can reach up to 1600 - 1700 K. Within this temperature range, slagging combustion can be realized. The temperature profiles in C1 and C2 are similar in most of the parts in the chamber. This is because the same inlet conditions for the air flow, which results in the similar aerodynamic field and combustion performance shown in Figure 2 to 4. For C1, there is a near-exit zone with a relatively lower temperature near the wall (marked with a red ellipse in Figure 5). Moreover, in the corner near the contraction part of C2, there is an area with a temperature peak of 2300K (marked with a blue ellipse in Figure 5), which indicating a large generating rate of thermal NOx in this place.

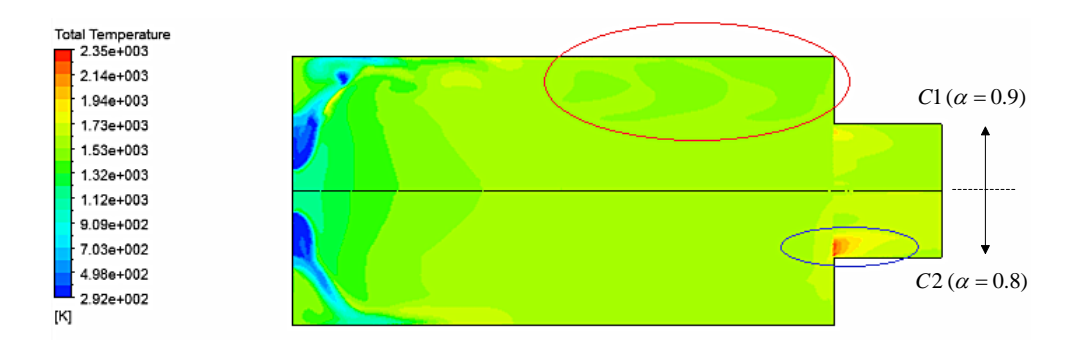


Figure 5. Contours of axial velocity (upper half, C1; lower half, C2)

The distribution of NO_x in the TSC chamber is shown in Figure 6. Here only thermal and fuel NO_x was calculated while prompt NO_x was ignored, considering the characteristics of the pulverized coal combustion. As is shown in Figure 6, NO_x is mainly generated in the near-axis regions downstream and the upper corner near the contraction part in C1; while for C2, NO_x is more evenly distributed along the radial direction. There is a NO_x concentration peak in the contraction part near the exit of C2 (highlighted in a blue ellipse in Figure 6). This is contributed by high thermal NO_x generation rate in this area, in accordance with the temperature peak shown in Figure 5.

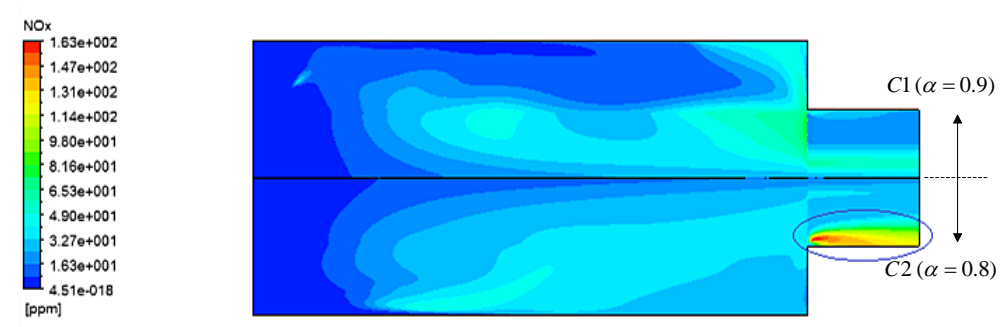


Figure 6. Contours of axial velocity (upper half, C1; lower half, C2)

	Particle Average	Average Volatile	Average Char
	Residence Time	Conversion Rate	Burnout Rate
	(s)	(%)	(%)
C1	1.00	99.61	93.52
C2	0.93	99.93	92.96
	Average	Average NO _x	Average NO _x
	Temperature in	Concentration Rate	concentration rate
	TSC Chamber	in TSC Chamber	@ exit
	(K)	(ppm)	(ppm)
C1	1472.75	21.47	25.89
C2	1516.54	23.21	71.46

Table 3 Summary of simulation results

Table 3 shows the combustion performance and the NOx generation rates under a fuel-rich condition of C1 and C2. The average particle residence time during combustion is around 1 s, which is favorable for highly efficient coal combustion. In both cases, the average volatile conversion rate is larger than 99.5%, and C1 yields a merely higher average char burnout rate of 93.52% to 92.96%. The average

temperature in the TSC chamber of C2 is about 45 K higher than that of C1. This is because with the same amount of combustion air and almost the same combustion efficiency, more burned coal means more heat is generated. Low NO_x combustion is realized for both cases, and C1 acquire a relatively lower NOx generation rate. The evenly distributed temperature profile in the chamber, along with the reducing atmosphere greatly inhibits the NO_x generating rate during the pulverized coal combustion. The average NO_x concentration rate near the exit for C1 is only 25.89 ppm, compared with 71.45 ppm for C2.

Conclusions

In this paper, the thermodynamics properties of a Twin Swirl Combustor (TSC) burning pulverized coal were studied. Simulation results show that the pulverized coal is burnt efficiently, with an average volatile conversion rate of larger than 99.5% and an average char burnout rate of 93%. Meanwhile, the NOx generation rate is reduced in a low level in the chamber. C1 with the stoichiometric ratio of 0.9 yielded lower NOx emission rates near combustor exit while remained high volatile conversion rate and char burnout rate, as compared with C2 with the stoichiometric ratio of 0.8.

Two swirling airflows in the chamber form strong swirling and recirculation zones. The particle residence time in the chamber is prolonged for around 1 s, which is beneficial for the highly efficient coal combustion. Most of the coal particles are burned in the vicinity of chamber wall. The increased wall temperature is favorable for ash deposition and molten slag discharge. An evenly distributed temperature profile as well as the fuel rich environment in the TSC chamber can further inhibit NOx generation during pulverized coal slagging combustion.

A detailed measurement of the thermal properties in the TSC is essential to further compare and evaluate the performance of the TSC and is expected to be conducted soon.

Acknowledgement

This work is supported by Funding of Jiangsu Innovation Program for Graduate Education (CXLX11_0193).

References

- Liu, Y. L. and Tang H. (2014) Numerical study on the interaction mechanism between swirl and reverse flow rate in a twin swirl combustor, *Advance Materials Research* **960-961**, 341-348.
- Müler, M., Lemp, O., Leiser, S., Schnell, U., Grathwohl, S., Maier, J., and Mönckert, P. (2010). Advanced modeling of pulverized coal combustion under oxy-fuel conditions. In *The 35th International Technical Conference on Clean Coal and Fuel Systems. Clearwater, FL*.
- Yakhot, V. and Orszag S. A. (1986) Renormalization group analysis of turbulence. I. Basic theory, *Journal of Scientific Computing* 1, 1-51.
- Kobayashi, H., Howard, J. B., and Sarofim, A. F. (1976) Coal devolatilization at high temperatures. In *Symposium (international) on combustion, Cambridge, Massachusets.*
- Smoot, L. D., & Smith, P. J. (1985). *Coal combustion and gasification*, Plenum Press, New York, USA. Raithby, G. D. and Chui, E. H. (1990). A finite-volume method for predicting a radiant heat transfer in enclosures with participating media. *Journal of Heat Transfer*, **112**(2), 415-423.
- Zhou, H., Yang, Y., Liu, H. Z. and Hang, Q. J. (2014) Numerical simulation of the combustion characteristics of a low NOx swirl burner: Influence of the primary air pipe, *Fuel* **130**, 168-176.
- Zeldovich, Y. B. (1946) The oxidation of nitrogen in combustion and explosions. *Acta Physicochim. URSS*, **21**(4), 577-628.